Numerical modelling of thermal convection related to fracture permeability in Dinantian carbonate platform, Luttelgeest, the Netherlands

Lindsay Lipsey[1,2], Jan-Diederik van Wees[1,2], Maarten Pluymaekers[1], Sierd Cloetingh[2]

[1] TNO, PO Box 80015, 3508 TA Utrecht, The Netherlands

[2] Utrecht University, PO Box 80.021, 3508 TA Utrecht, The Netherlands

lindsay.lipsey@tno.nl

Keywords: Thermal convection, 3D numerical modelling, Temperature anomaly

ABSTRACT

We reproduce the thermal gradient at the Luttelgeest-01 (LTG-01) in the northern onshore region of the Netherlands using 3D numerical models in order to better understand the interplay between natural fracture permeability and temperature patterns. Numerical models of thermal convection are used to illustrate the role of permeability on the timing of convection onset, convection structure development and resulting temperature patterns.

1. INTRODUCTION

Thermal anomalies in deep sedimentary layers and basement rock are largely controlled by convective fluid flow within permeable zones. Convection is of interest in geothermal energy, as upwelling hot fluid yields relatively shallow high-temperature anomalies. These are preferential targets for geothermal exploration. Convective fluid flow leaves a distinct pattern on the local geothermal gradient. The thermal effect is critically dependent on the pre-existing thermal gradient, thickness and permeability (e.g. Pasquale et al., 2013) (Lipsey et al., 2016).

Recent work on the temperature distribution in the Dutch subsurface revealed a thermal anomaly at 4-5 km depth at Luttelgeest-01 (LTG-01), which could be explained by thermal convection. Temperature measurements show a shift to higher temperatures at depths greater than 4000 m, corresponding to the Dinantian carbonate interval. The local thermal gradient strongly resembles the thermal signature that is believed to be characteristic of convective processes (Lipsey et al., 2016).

The aim of this research is to use 3D numerical models of thermal convection to reproduce the temperature pattern in Luttelgeest, in order to illuminate possible flow and thermal structures. The goal is to gain a better understanding of the interplay between geothermal anomalies, platform geometry and natural permeability. Numerical models are used to test the effect of platform geometry on the development of thermal convection and resulting temperature patterns (Lipsey et al., 2016).

2. GEOLOGICAL SETTING

During the Carboniferous, the Netherlands was part of a large intra-cratonic basin known as the Northwest European Carboniferous Basin (NWECB) (Kombrink et al., 2010). The basin is delineated by the Mid north Sea High to the north and the London-Brabant Massif to the south. It formed in response to renewed back-arc extension in the Rhenohercynian basin, which occurred following the Caledonian orogeny during mid-Devonian times. This initiated the formation of a series of linked NW-SE trending fault blocks. During the Dinantian the Netherlands part of the NWECB experienced a tensional regime, resulting in a horst-and-graben complex (Kombrink et al., 2010) (Kombrink, 2008) (Lipsey et al., 2016) (Fig. 1).

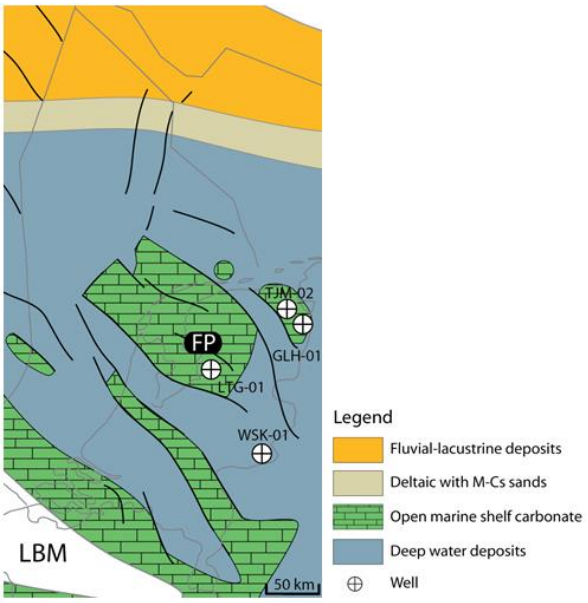

Figure 1: Paleogeographic map of the Netherlands during the Early Carboniferous. LBM: London-Brabant Massif; FP: Friesland Platform (Lipsey et al., 2016).

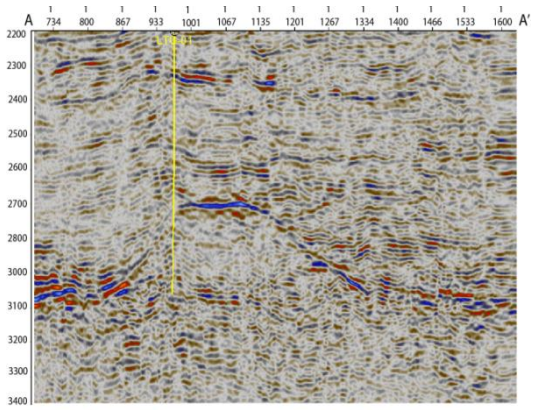

Figure 2: Seismic section across the Luttelgeest platform. The LTG-01 well is indicated in yellow. Note the location of the well along the platform of the margin (Lipsey et al., 2016).

The LTG-01 well is located on the Luttelgeest carbonate platform, which is found on the Texel-Ijsselmeer structural high. This is a prominent NW-SE trending fault block of mid-Palaeozoic origin (Fig. 1) (Geluk et al., 2007). The southern boundary is made up of a steep fault system and the northern margin gradually transitions into the adjacent Friesland platform. The Luttelgeest carbonate platform is elongated in the E-W direction, with dimensions of approximately 14 km E-W and 8 km N-S (Lipsey et al., 2016). The seismic profile in Fig. 2 shows the relative position of the LTG-01 well, which appears to be situated on the edge of the platform, or platform margin (Lipsey et al., 2016). This is in agreement with other seismic studies of the Luttelgeest platform (e.g. van Hulten and Poty, 2008)

3. EVIDENCE FOR CONVECTION

3.1 Temperature

Bonté et al. (2012) provides the most recent up-to-date coherent temperature dataset for the Netherlands. In total, the dataset includes 1293 corrected bottom-hole temperature measurements (BHT) distributed over 454 wells and yields an average gradient of 31.3 °C km^{-1} with a mean surface temperature of 10.1 °C (Fig. 3). However, there is a sudden shift in the data towards high temperatures at depths greater than 4 km, as indicated by the dashed line in Fig. 3a. These anomalous high values at great depth correspond to the following deep wells: LTG-01, TJM-02, WSK-01 and GLH-01 (Lipsey et al., 2016).

For a better understanding of subsurface temperatures, Bonté et al. (2012) use this dataset to calibrate 3D thermal models for the complete Dutch subsurface. The comparison between the model and the values within a 10km radius of the LTG-01 well is shown in Fig. 3b (Bonté et al., 2012).

The dataset for LTG-01 yields a temperature gradient of 39 °C km^{-1} though contains several intervals of anomalous values. Within the platform, the gradient is nearly 10 °C km^{-1} lower than the Dutch average, whereas above the platform the gradient is roughly 20 °C km^{-1} higher. Such a decrease in the temperature gradient through the platform is typical of a convective signature resulting from hot upwelling fluid (Guillou-Frottier et al., 2013) (Lipsey et al., 2016).

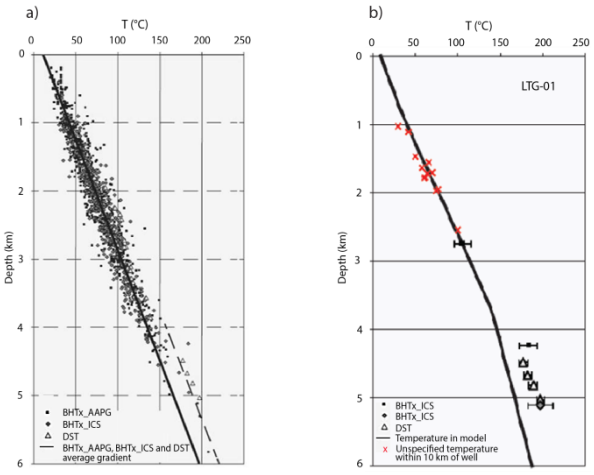

Figure 3: (a) Temperature vs. depth for the Dutch (b) Comparison between values used as calibration and modelled temperature for LTG-01 (Bonté et al., 2012)

3.2 Permeability assessment

Permeability was calculated by TOTAL from wireline pressure tests and reported in the composite log (report accessible from www.nlog.nl). The permeability values range from 10 to 598 mD (10-14 to 6 10-13 m2), however several measurements were registered as fair or questionable (Lipsey et al., 2016). Van Oversteeg et al. (2014) calculated the permeability and transmissivity based on mud losses and proposed that there is an interval with fracture permeability between 4550 to 5150 m. For a reservoir thickness of 600 m, an overall permeability of 6 10^{-14} m^2 was calculated (Van Oversteeg, 2014). This value is in accordance with the permeability range inferred from pressure measurements, but should be taken with caution as the permeability is not equally distributed throughout the entire interval of 600m. For example, between 4800 and 4975 m there is no evidence of permeability. An overview of the permeability assessment is presented in Table 1 (Lipsey et al., 2016).

Table 1: Overview of results from permeability assessment

Source/method	Depth interval	Permeability
Composite well log	Some intervals of increased permeability	
Wireline Pressures	4535 – 4647 m	10^{-14} – 6 10^{-13} m^2
Rock samples	4378 – 4473 m	2 10^{-16} – 9 10^{-15} m^2
Mud losses	600 m	> 10^{-12} m^2

4. METHODS

4.1 Governing equations

The numerical study of thermal convection in permeable and porous media involves the coupling of heat transfer and fluid flow equations that incorporate

realistic fluid and rock properties. In a Eulerian reference framework, the heat equation is written as

$$\rho c \frac{\partial T}{\partial t} = \nabla \cdot (\lambda \cdot \nabla T) - \vec{v} \cdot \nabla T \quad [1]$$

See Table 2 for nomenclature. The advective velocity can also be a result of fluid flow inside pores or fractures which can strongly affect the thermal distribution (e.g. Guillou-Frottier et al., 2013; Cherubini et al., 2014). The fluid velocity is resolved from solving the Darcy flow equation:

$$c_h \frac{\partial P}{\partial t} = \nabla \cdot \left(\frac{k}{\mu} \left(\nabla P + \frac{(\rho_f - \rho_0)}{\rho_0} g \nabla z \right) \right) + Q \quad [2]$$

See Table 2 for nomenclature. Through solving the pressure field in equation [4], the velocities can be determined as

$$\overrightarrow{v_f} = \frac{k}{\mu} \left(\nabla P + \frac{(\rho_f - \rho_0)}{\rho_0} g \nabla z \right) \quad [3]$$

And can be incorporated in equation [1] by adopting:

$$\vec{v} = \varphi \frac{\rho_f c_f}{\rho c} \overrightarrow{v_f} \quad [4]$$

Temperature dependent density and fluid dynamic viscosity have been used. For the details of the equations, refer to Lipsey et al. (2016).

Table 2: Nomenclature for model equations

Symbol	Name	Unit
ρ	Bulk density of porous rock	kg m^{-3}
ρ_f	Fluid density	kg m^{-3}
ρ_0	Reference density	-
C	Bulk specific heat capacity	J kg^{-1} K^{-1}
C_f	Specific heat capacity of fluid	J kg^{-1} K^{-1}
C_h	Bulk hydraulic storage capacity	m^3 Pa^{-1}
g	Gravitational acceleration	m s^{-2}
T	Temperature	°C
t	Time	s
P	Pressure	Pa
μ	Fluid viscosity	Pa s
λ	Thermal conductivity	W m^{-1} K
Q	Source term	m^3 s^{-1}

4.2 Geometry and boundary conditions

Three-dimensional coupled fluid and heat transport models are simulated using a numerical solver developed in a Java programming language. Temperature at the top of the model is 10 °C and 244 °C at the bottom reflecting a linear thermal gradient of 39 °C km^{-1}. All boundaries of the platform are impermeable, defining a closed system with no sources or sinks for the fluid. Lateral boundaries are thermally insulating. Rock thermal properties are assumed to be uniform for the entire model.

Experiments begin with an initial perturbation to the conductive temperature field by injecting cold fluid into the platform. During computation, the initial conductive field evolves towards steady-state convection within a few thousand years, therefore simulations run for 500k years.

4.3 Model scenarios

Two platform geometries are tested. The first geometry, referred to as model 1, is characterized by a flat platform base, where the thickness of the inner platform is 800 m. In the second geometrical configuration (model 2) the shape of the platform top remains the same, however the base of the platform is curved upwards. In order to keep the thickness of the inner platform at 800 m, the thickness of the margins is increased by 400 m, extending down to 5600 m depth at the platform margin. Fig. 4 provides an overview of the model geometries (Lipsey et al., 2016).

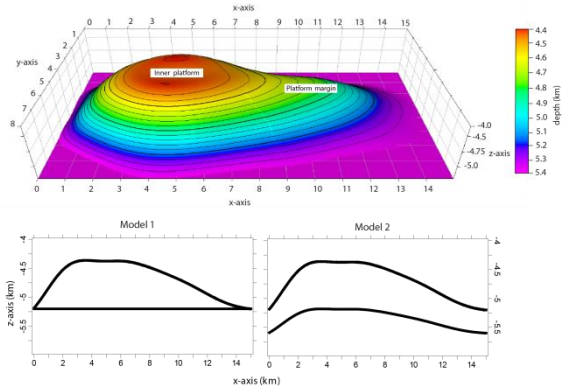

Figure 4: Geometry of platform. Bottom: cross sections showing the different geometries in model 1 and model 2 (Lipsey et al., 2016).

5. RESULTS

5.1 Convection cell structure

In this paper, we present the results for a permeability of 2 10^{-14} m^2 (subscript a) and 6 10^{-14} m^2 (subscript b), which are applied to both geometric scenarios (models 1a,1b, 2a,2b).

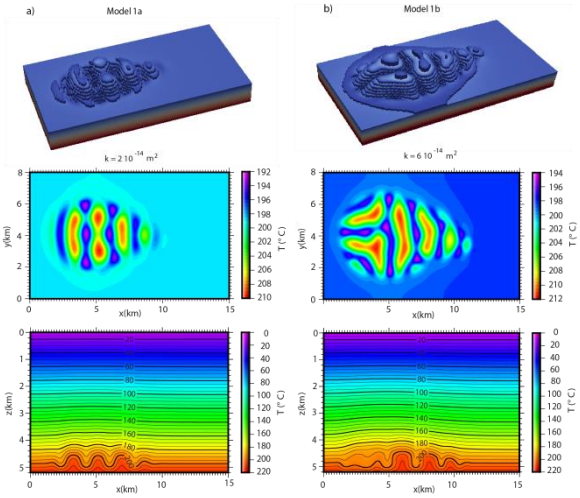

Figure 5: Results for model 1a and 1b. Top: 3D view of the modelled temperature field. Middle: Temperature on horizontal plane at z=4.8 km. Bottom: Cross section at y=4km (Lipsey et al., 2016).

Model 1a relaxes into a steady-state eight cell convection pattern, characterized by four dominant upwelling plumes. Model 1b relaxes into a more complex convection pattern, characterized by four elongate polyhedral shapes. The upwelling plumes are concentrated in the thickest part of the platform in both model 1a and 1b (Fig. 5) (Lipsey et al., 2016).

Models 2a and 2b, where the base geometry of the platform changes from flat to upward curving, steady-state convection is reached sooner. Model 2a relaxes into a structure that is a combination of circular and elongated shaped upwellings, whereas model 2b is dominated by a more circular upwelling pattern with an increased number of convection cells (Fig. 6)

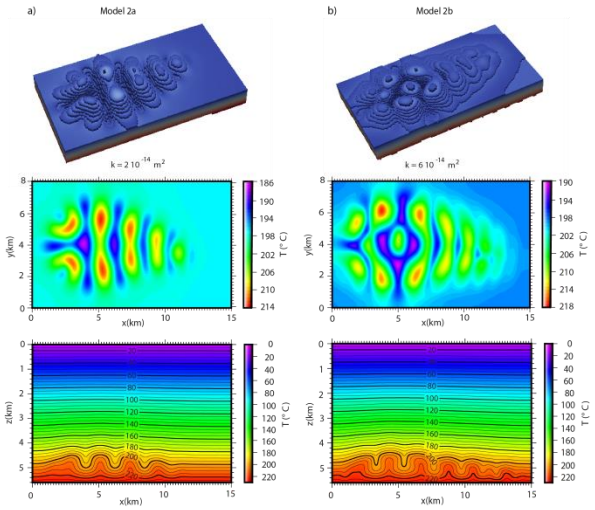

Figure 6: Results for model 2a and 2b. Top: 3D view of the modelled temperature field. Middle: Temperature on horizontal plane at z=4.8 km. Bottom: Cross section at y=4km (Lipsey et al., 2016).

5.1 Convection cell structure

Fig. 7 shows how convective fluid flow effects the temperature field in models 1 and 2. The measured temperature values from within the platform in well LTG-01 have been added for reference. Geothermal gradients have been measured along the axis of three points in each model: downwelling, mixing zone and upwelling (Lipsey et al., 2016).

The gradient is steepest along the axes of upwelling, which results in relatively low gradients through the platform. The gradient is as low as 13°C km^{-1} in model 2b, where the platform has both a large permeability and thickness. As models have matching thermal boundary conditions, the temperature oscillates around the same temperature (200 °C) at mid-depth.

While the temperature data set from the LTG-01 well does suggest that the average gradient is elevated with respect to the Dutch average gradient of 31 °C km^{-1}, it appears that applying a gradient of 39 °C km^{-1} causes an over enhancement of temperatures once convection stabilizes within the carbonate platform reservoir. We therefore adjust the boundary conditions such that the gradient is no longer elevated. The temperature enhancement relative to the conductive profile is similar to the previous models. As the geothermal gradient is now lower, the maximum temperatures attained within regions of upwelling are lower, ranging from 182 °C in model 1a to 192 °C in model 2b. These temperatures more comparable with the measured temperature values at LTG-01 well.

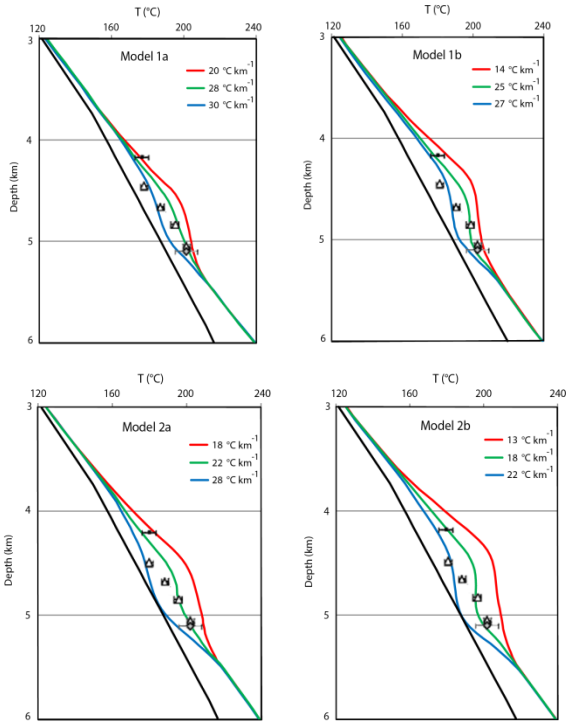

Figure 7: Modelled profiles along three axes: upwelling (red), mixing zone (green) and downwelling (blue). Measured temperature data from LTG-01 included for comparison. Black curve represents measured geothermal gradient (Lipsey et al., 2016).

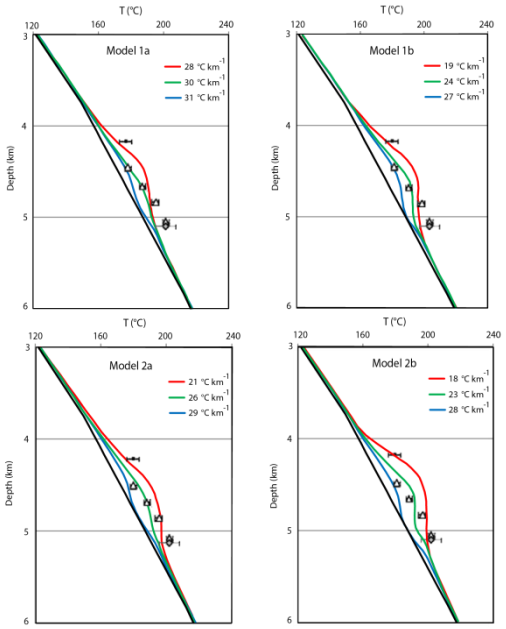

Figure 8: Modelled profiles for a non-elevated gradient. See Fig. 7 for explanation of curves.

5. CONCLUSIONS

This study investigates the potential for thermal convection in the Luttelgeest carbonate platform. We use 3D numerical models of thermal convection to reproduce the thermal gradient at LTG-01 well. Numerical experiments test the effect of platform geometry and permeability on the development of thermal convection and resulting temperature patterns (Lipsey et al., 2016).

Convective upwellings can create significant temperature enhancements relative to the conductive profile and in agreement with the observations in the Luttelgeest carbonate platform. This enhancement is critically dependent on the platform geometry and permeability structure (Lipsey et al., 2016). Furthermore, numerical models show that the spacing of convective upwellings, and therefore spacing of thermal anomalies, can be predicted theoretically by knowing the platform thickness and permeability. The strong spatial variability of thermal anomalies in convective fractured aquifers at large depth can have a strong effect on exploration opportunity and risk of prospective areas. Numerical models can facilitate in exploration workflows to assess thermal variation and location of upwelling zones (Lipsey et al., 2016).

REFERENCES

Bonté, D., Van Wees, J.-D., and Verweij, J. M.: Subsurface temperature of the onshore Netherlands: new temperature dataset and modelling, Geol. Mijnbouw-N. J. G., 91, 491–515, 2012.

Cherubini, Y., Cacace, M., Scheck-Wenderoth, M., and Noack, V.: Influence of major fault zones on 3-D coupled fluid heat transport for the Brandenburg region (NE German Basin), Geoth. Energ. Sci., 2, 1–20, 2014.

Geluk, M.C., Dusar, M., and de Vos, W.: Pre-Silesian, in: Geology of the Netherlands, Royal Netherlands Academy of Arts and Sciences, Amsterdam, the Netherlands, 27–42, 2007.

Guillou-Frottier, L., Carré, C., Bourgine, B., Bouchot, V., and Genter, A.: Structure of hydrothermal convection in the Upper Rhine Graben as inferred from corrected temperature data and basin-scale numerical models, *J. of Volcanol. Geoth. Res.*, 256, 29–49, 2013.

Kombrink, H.: Tectonics and sedimentation in the Northwest European Carboniferous Basin, in: The Carboniferous of the Netherlands and surrounding areas; a basin analysis, PhD Thesis, Universiteit Utrecht, 21 – 46, 2008.

Kombrink, H., Van Lochem, H., and Van der Zwan, K.J.: Seismic interpretation of Dinantian carbonate platforms in the Netherlands; implications for the palaeogeographical and structural development of the Northwest European Carboniferous Basin, *J. Geol. Soc.*, 167, 99–108, 2010.

Lipsey, L., Pluymaekers, M., Goldberg, T., van Oversteeg, K., Ghazaryan, L., Cloetingh, S., and van Wees, J.D.: Numerical modelling of thermal convection in the Luttelgeest carbonate platform, the Netherlands, *Geothermics*, 64, 135-151, 2016.

Pasquale, V., Chiozzi, P., and Verdoya, M.: Evidence for thermal convection in the deep carbonate aquifer of the eastern sector of the Po Plain, Italy, *Tectonophysics*, 594, 1–12, 2013.

Van Hulten, F.F.N., and Poty, E.: Geological factors controlling Early Carboniferous carbonate platform development in the Netherlands, *Geol. J.*, 43, 175–196, 2008.

Van Oversteeg, K., Lipsey, L.C., Pluymaekers, M., van Wees, J.-D., Fokker, P.A., and Spiers, C.J.: Fracture Permeability Assessment in Deeply Buried Carbonates and Implications for Enhanced Geothermal Systems: Inferences from a Detailed Well Study at Luttelgeest-01, The Netherlands, in Proceedings Thirty-Eighth Workshop on Geothermal Reservoir Engineering, Stanford University, Stanford, California, 2014.

Acknowledgements

The research leading to these results has received funding from the European Community's Seventh Framework Programme under grant agreement No. 608553 (Project IMAGE).